Potato quality assessment by monitoring the acrylamide precursors using reflection spectroscopy and machine learning

Smeesters, Lien; Magnus, Indy; Virte, Martin; Thienpont, Hugo; Meulebroeck, Wendy

Published in:
Journal of Food Engineering

DOI:
10.1016/j.jfoodeng.2021.110699

Publication date:
2021

Potato quality assessment by monitoring the acrylamide precursors using reflection spectroscopy and machine learning

L. Smeesters [a,b], I. Magnus [a,b], M. Virte [a], H. Thienpont [a,b], W. Meulebroeck [a,b]

[a] Vrije Universiteit Brussel, Department of Applied Physics and Photonics, Brussels Photonics (B-PHOT), Pleinlaan 2, B-1050 Brussels, Belgium

[b] Flanders Make, Pleinlaan 2, B-1050 Brussels, Belgium

* Corresponding author: lsmeeste@b-phot.org (+32 2 629 18 14)

Abstract

Acrylamide formation is nowadays one of the major concerns of the potato-processing agriculture industry. We investigate the use of broadband reflection spectroscopy (400 – 1700 nm), in combination with machine learning, to optically classify raw potatoes inducing different levels of acrylamide after frying, covering concentrations between 200 ppb and 2000 ppb. Using the full spectral range, we obtain a correct classification of a dataset of 200 samples and using 10-fold cross-validation, while applying Linear Discriminant Analysis and Extreme Learning Machine. To reduce the amount of data and increase processing speeds, a sequential feature selection search was performed to identify the critical wavelengths (450 nm, 488 nm, 504 nm, 783 nm, 808 nm, 1310 nm, 1319 nm and 1342 nm) that enable classification performances exceeding 92 % when applying Linear Discriminant Analysis. We therefore demonstrate a non-destructive identification of the potatoes unsuited for French fries production, enabling to increase food safety, while limiting food waste.

Keywords: reflection spectroscopy, acrylamide, potato, optical sensing, linear discriminant analysis, machine learning

1. Introduction

Acrylamide is a 2A-classified carcinogenic chemical that forms during high-temperature processing (>120°C) of starch-rich food products, as potatoes, cereals and coffee (EFSA, 2015; Mottram et al., 2002). It forms as a side

product of the Maillard reaction, during which reducing sugars and asparagine interact and which contributes to the browning, flavor and aroma of the food products. To limit the human acrylamide exposure, the European Commission provides toolboxes raising awareness on the reduction of acrylamide in manufacturing processes and identifies benchmark acrylamide levels for a number of food categories, as French fries, crisps, breakfast cereals and coffee (European Commission, 2017). For ready-to-eat French fries an indicative limit of 500 ppb was defined. To compare the contamination level of the French fries with these recommendations, the acrylamide concentrations are nowadays determined using chemical analysis, like liquid chromatography – tandem mass spectrometry (LC-MS/MS). Despite the guidelines, high acrylamide concentrations (up to 3240 ppb) are still reported in potato-based food (Mousavi Khaneghah et al., 2020), indicating the need for continuous development of novel acrylamide sensing technologies.

To increase food safety while minimizing food waste, we focus on the potato quality evaluation and acrylamide precursors concentration prior to frying. As such, the potatoes unsuited for frying can still be used for low-temperature processing, like mashed potatoes and potato soup. Within industry, the quality of raw potatoes is currently mainly evaluated by underwater weight tests. However, until now, no consistent relationship between the underwater weight and acrylamide formation could be established (Brunt et al., 2010; Helgerud et al., 2012). In addition, several best practice guidelines are being applied to minimize the acrylamide formation, as for example a reduction of the frying temperature, an optimization of the storage conditions, the use of thicker fries and the application of pre-treatment techniques with chemical or natural additives (De Wilde et al., 2005; Gökmen et al., 2006; Jung et al., 2003; Medeiros et al., 2012; Morales et al., 2014; Pedreschi et al., 2007). However, as a main drawback, these methods influence the colour, taste and structure of the resulting French fries.

We pursue a non-destructive optical detection of raw potatoes susceptible to an excessive acrylamide formation during frying. Specifically, we target the use of ultraviolet – visible – near-infrared (UV-VIS-NIR) reflection spectroscopy to obtain an accurate identification of the potatoes unsuited for frying, minimizing the amount of French fries containing acrylamide concentrations above 500 ppb in the food chain, without affecting the taste, structure or composition of the French fries. The composition of potatoes is already widely investigated by the use of visible and near-infrared spectroscopy (Helgerud et al., 2015; Rady et al., 2014; Subedi and Walsh, 2009). Rady et al. used the 446 – 1125 nm spectral range to sense glucose and sucrose in potato tubers. Helgerud et al. and Subedi et al. illustrated the monitoring of the dry matter content, using the 449 – 1040 nm and the 750 – 950 nm spectral range respectively. In addition, all acrylamide precursors show clear absorption

characteristics, indicating optical spectroscopy as a promising detection method. Water typically has a high absorbance around 1400 – 1490 nm (Büning-Pfaue, 2003; Curcio and Petty, 1951), starch has a high absorbance around 1200 nm (Lopez et al., 2013; Nawrocka and Lamorska, 2013), reducing sugars have a high absorbance around 800 – 1000 nm and 2100 – 2500 nm (Ozaki et al., 2007; Rady et al., 2014), while asparagine shows a higher absorbance around 200 – 230 nm and 3000 – 4000 nm (National Institute of Standards and Technology, 2020). Despite these known spectra, connecting the absorption characteristics of the raw potatoes to the acrylamide formation after frying remains a challenging research question. In general, potatoes with slightly different compositions only show minor differences in their spectral characteristics, often hidden by the natural variation and harvest-dependent influences (soil, temperature, irrigation). In a preceding study, we presented the use of spatially resolved spectroscopy to identify potatoes giving rise to an excess of acrylamide, indicating a promising identification based on the separate measurement of NIR specular reflected and scattered light signals (Smeesters et al., 2017). Using this detection methodology, a clear separation could be obtained between the suitable and unsuitable potatoes for frying. However, this measurement configuration requires a high-power supercontinuum light source and a sensitive detector to capture the weak scattered light signals, imposing strict requirements for its industrial integration.

We propose an alternative approach to non-destructively identify raw potatoes that induce high acrylamide formation during frying, based on UV-VIS-NIR reflection spectroscopy in combination with machine learning, enabling to obtain a precise classification while limiting food waste and offering an easier integration in an industrial configuration. We demonstrate this approach by successfully classifying five different potato batches which led to different acrylamide concentrations after frying (200 ppb, 240 ppb, 640 ppb, 890 ppb, 2000 ppb). In general, spectroscopic data are traditionally processed using multivariate methods (Adedipe et al., 2016; Ayvaz et al., 2013; Pedreschi et al., 2010; Segtnan et al., 2006) such as Principal Component Analysis (PCA) and Partial Least Squares (PLS). More recently, an increasing interest is given to the application of non-linear machine learning techniques for the evaluation of food products, as for chicken meat evaluation (Barbon et al., 2018), peach variety detection (Rong et al., 2020) and the pectin content determination in orange juice (Bizzani et al., 2020). In this work, we investigate whether machine learning algorithms can improve the acrylamide monitoring and classification performance. Insight is given in the considered potato batches, the reflection spectroscopy measurement setup and data processing methodology (Section 2). First, the full UV-VIS-NIR reflection spectrum is considered during the processing of the data. Second, in view of data reduction and to obtain higher processing speeds, a processing algorithm based on a limited number of wavelengths is used, for which the most significant

wavelengths were defined using a sequential feature selection. In both cases, outstanding classification performances are obtained (Section 3), indicating a successful sensing of raw potatoes giving rise to an excessive acrylamide formation during frying.

2. Materials and methods

To accurately study the optical differences between raw potatoes giving rise to low (<500 ppb) and high (≥500 ppb) acrylamide concentrations during frying, the availability of reliable samples and the development of a sensitive measurement methodology are of major importance. In this section, we first give an overview of the investigated potato batches, after which we explain the operation of our developed reflection spectroscopic measurement configuration. Finally, the chemometrics and machine learning steps are described that are considered during the post-processing of the spectroscopic data.

2.1 Sample preparation

We investigate raw potatoes of the subtype Bintje (Solanum tuberosum L.), typically used for French fries production. To obtain reliable potato samples with a different acrylamide formation during frying, while ensuring an efficient and repeatable measurement procedure, we generated our own samples using optimized storage procedures. The potato samples inducing low acrylamide formation (samples A and B) were obtained by controlled storage of the potatoes in a farmer's root cellar, taking into account the best known practices for long-term potato storage, guaranteeing a good quality preservation of the fresh potatoes (Linsinska and Leszczynski, 1989; Voss et al., 2015). Potato samples susceptible to the formation of high acrylamide contents during frying were artificially created by storage of different potato batches at 4°C, all of which originated immediately from the farmer and were obtained shortly after the harvest. According to previous research, the latter storage procedure influences the acrylamide precursors, inducing a boost in the acrylamide formation, depending on the storage time (De Wilde et al., 2005; Hebeisen et al., 2007; Matsuura-Endo et al., 2006). Samples C, D and E were obtained after 12, 22 and 28 weeks of storage, giving rise to increasing acrylamide precursor concentrations. Samples A and E were originating from the same field and harvest, as well as samples B, C and D. A total of 200 potatoes were considered in this study, of which 17 in sample A, 15 in sample B, 12 in sample C, 136 in sample D and 20 in sample E. No potato samples from the supermarket were considered, since we target to apply our sensing

technology immediately after the harvest. The potatoes that are offered in the supermarket are already quality screened using underwater weight tests, thus giving no complete view on the natural variation of the potato samples after the harvest.

The reflection spectroscopy measurements were performed on freshly cut fries, immediately after peeling and cutting. The potatoes were cut with a fry cutter, in a cuboid shape with a height and thickness of 9 mm and a length between 20 mm and 90 mm, depending on the size of the potato tuber. After performing the non-destructive spectroscopy measurements, the concentration of acrylamide precursors in the raw potatoes and the corresponding acrylamide content in the French fries were determined using chemical analysis, which were outsourced to SGS, a company specialised in testing and certification. In both the potatoes and the French fries, the fructose, glucose and asparagine concentration were measured using high-performance liquid chromatography, while the starch concentration was determined using Ewers method and the moisture concentration was measured with a dehydrator. In addition, for the French fries, the acrylamide concentrations are determined using LC-MS/MS. The French fries were obtained by frying the potatoes using a 2000 W fryer with 3.5 l natural frying oil, while following the procedure explained by De Wilde et al.. The cut potatoes were fried in a 2-stage frying process: during the first stage, the potatoes were fried for 3 minutes at 180°C, while during the second stage, they were fried for 2 minutes at 180°C. In-between both frying stages, the fries were cooled down for 10 minutes at room temperature (De Wilde et al., 2005).

2.2 Reflection spectroscopy measurement setup

The reflection spectra of the potatoes were measured independently of the reflection angle or surface scattering using a reflection integrating sphere (AvaSphere-30 of Avantes). The integrating sphere contains a single sample port, on which the potato can be positioned, and two fibre connectors to connect the illumination light source and the detection optical spectrum analyser (Figure 1). For the illumination of the sample, we use a combination of deuterium and halogen pigtailed light sources, emitting light from 200 nm to 2500 nm, enabling to study the UV, visible and NIR spectral region. To direct the illumination light bundle to the integrating sphere, the end of the pigtailed source fibre is coupled into the illumination fibre (Avantes FC-UVIR600-2) via the use of an SMA-terminated collimating lens, enabling a light coupling efficiency of > 90%. The illumination fibre is connected to the sample port of the integrating sphere, illuminating a surface area of 28.3 mm² under an angle of 8° (to avoid

back reflections). All reflected light of the sample is subsequently collected by the integrating sphere, which is coated with a 98 % diffuse reflective coating ensuring that all collected light enters the detection fibre (Avantes FCB-UVIR600-2) guiding the light to the spectrum analyser. The spectrum analyser consists of two different channels with linear detector arrays simultaneously measuring the UV, visible and NIR light. The first channel contains the Avantes AvaSpec3684 spectrometer, able to measure the optical spectrum between 200 nm and 1100 nm with a resolution of 1.4 nm. The second channel contains the Avantes AvaSpec256 spectrometer, enabling to measure the spectrum between 1000 nm and 1700 nm, with a resolution of 4 nm.

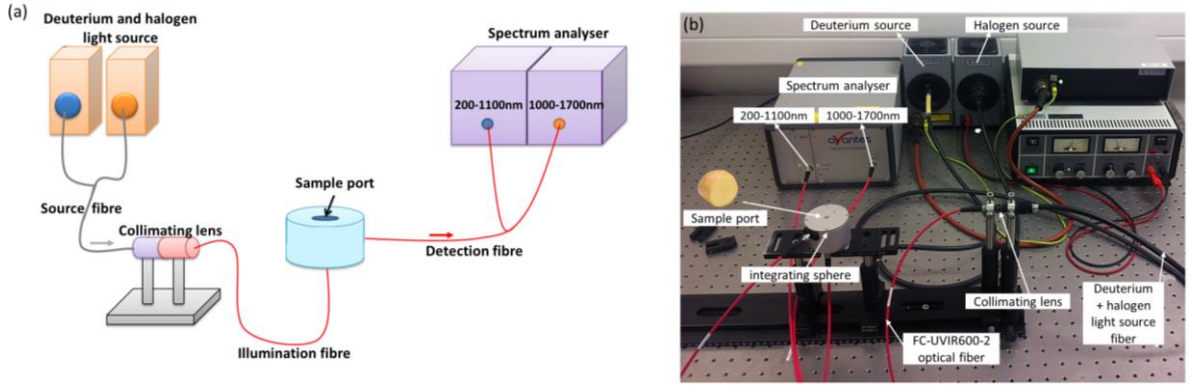

Figure 1: Reflection spectroscopy measurement configuration:

(a) schematic of the measurement setup; (b) general overview of the lab setup.

Prior to the reflection measurements, the reference and dark spectrum were determined. The reference spectrum, corresponding to the source spectrum, was measured after positioning a calibrated 99.9 % reflective tile (Spectralon® diffuse reflectance standard SRS-99-10) at the sample port of the integrating sphere. The dark spectrum was obtained by measuring the light intensity in case no sample is present at the sample port of the integrating sphere, measuring the illumination light that might reach the spectrum analyser without reflections on the sample. Next, the reflectance of the potato samples is calculated as the ratio of the reflected light intensity on the sample and the reference spectrum, both corrected for the dark spectrum. All measurements were performed in a dark environment, without the presence of ambient light, to maximize the dynamic range.

2.3 Chemometrics and Machine Learning

The measured reflection spectra are processed using chemometrics and machine learning data processing techniques, targeting to design a multi-class classifier able to distinguish 5 classes corresponding to the 5 distinct potato batches described earlier that induce different acrylamide concentrations after frying. In a first stage, the whole reflection spectrum is used as input for the post processing. Second, a reduction of the number of wavelengths is considered, to limit the processing time and ease the implementation in an industrial setting. Particularly, the reflectivity at specific commercially available laser lines are taken into consideration.

In general, different steps are followed during the processing of the spectroscopic date. First, pre-processing of the data is executed, including normalization and smoothing. Second, a multi-class classifier is trained, after which an evaluation of the classification is performed. The *Statistics and Machine Learning* toolbox of MATLAB® was used to process the data.

2.3.1 Broadband spectral evaluation

To obtain an optimal classification of the potato batches, different pre-processing and classification algorithms were studied and compared. Pre-processing of the raw spectroscopic data is crucial in obtaining satisfying classification results (Gautam et al., 2015; Gorry, 1990). Therefore, 7 classical techniques, and their combinations, were implemented and compared: (1) no pre-processing, (2) standard normal variate (SNV), (3) multiplicative scattering correction (MSC), (4) Savitsky-Golay (SG) filtering, (5) 1st derivative of SG, (6) 2nd derivative of SG and (7) feature standardization (FS). The SG filtering was applied using a 3rd order polynomial and window size of 101 points in the UV-VIS region and 11 points in the NIR region. The polynomial order and window size were carefully chosen to decrease the noise, but without affecting the underlying signal characteristics. A larger window size was considered for the UV-VIS region than for the NIR region, in correspondence with the measurement resolution.

In the next step, different classifiers were trained. All available data are used as training data, without the use of an external hold-out set, while the evaluation is done using repeated cross validation. Particularly, ten stratified fold cross-validation was used to create the training and validation sets. We considered 10 of the most popular chemometric and machine learning techniques (Gautam et al., 2015; Zareef et al., 2020), being Naïve Bayes (NB),

Linear Discriminant Analysis (LDA), Quadratic Discriminant Analysis (QDA), Support Vector Machine (SVM), Extreme Learning Machine (ELM), K-Nearest Neighbours (KNN), Decision Tree (DT), Random Forest (RF), Boosted Tree (BT), Partial Least Squares (PLS) and Neural Network (NN). The LDA was trained using a regularized, pooled covariance matrix, while QDA used the pseudoinverse of the covariance matrix. The SVM used the one-vs-one approach and the radial basis function as a kernel, with the box-constraint as hyperparameter. The ELM was operated with randomly assigned weights for the hidden layer, using 50 neurons together with the rectified linear unit (ReLU) as activation function and a regularization factor of 10^{-2}. To reduce the effect of the randomly assigned weights, an ensemble of 10 ELM classifiers was formed. The KNN used the Euclidean distance and number of neighbours as hyperparameter. The tree-based classifiers were trained using the Gini impurity, with the maximum number of splits and learning rate as hyperparameter for the DT and BT respectively. The RF and BT used 100 trees with 15 and 5 maximum splits each. The PLS classifier used binary encoding for the different classes and the number of principal components as hyperparameter. The NN analysis was executed using 100 neurons in the hidden layer and a sigmoid as activation function. A grid search was used to find the optimal hyperparameters of the classifiers.

Finally, evaluation was performed using 10-fold cross validation, in combination with a receiver operating characteristics (ROC) curve metric (Brownlee, 2014). More precisely, an extension of the ROC used in binary problems was used as metric, based on the misclassification rates (MCR) of each class. A ROC value equal to zero is targeted, meaning that all samples are correctly labelled, thus corresponding to an accuracy of 100 %.

$$ROC = \sqrt{\sum_{k=1}^{5}(MCR_k)}^{\,2} \tag{1}$$

$$\text{With } MCR_k = 1 - \frac{CM(k,k)}{\sum_{i=1}^{5} CM(k,i)} \tag{2}$$

and CM the 5x5 confusion matrix, of which each row represents the actual class and each column the predicted class, and the numbers in the matrix correspond with the classification rate. In case all samples are correctly classified, this corresponds to a diagonal matrix.

2.3.2 Selected wavelengths evaluation

After investigation of the performances using all data available and to increase the computation speed, we focused on data reduction techniques, enabling to obtain an as good as possible classification performance when only considering a limited number of features; that is, here, a limited number of wavelengths of the reflectance measurement. In this work, the classification is optimized when limiting the total number of wavelengths to 8 commercially available laserlines, to enable the potential integration into industrial optical sorting machines.

In a first step, the original broadband spectral data matrix (200 x 605) is downscaled to 200 x 18 by only considering 18 common commercially available laser wavelengths, being: 405 nm, 450 nm, 488 nm, 505 nm, 520 nm, 532 nm, 633 nm, 660 nm, 783 nm, 808 nm, 830 nm, 850 nm, 1030 nm, 1064 nm, 1310 nm, 1319 nm, 1342 nm and 1550 nm (Integrated Optics, 2020). Furthermore, to obtain a stable detection criterion, eliminating the influence of environmental changes that might be present in an industrial setting, e.g. variable object distance and laser power variations, the reflectance ratios will be used instead of the raw values. This results in 306 possible ratios, giving rise to a modified 200 x 306 data matrix. No other pre-processing or data transformation is applied.

As a second step, the feature selection is applied, targeting to reduce the number of wavelengths from 18 to 8, while determining the most important reflectivity ratios. Since the feature selection only needs to be executed once and the best performance was targeted, the greedy sequential forward selection (SFS) search was used, which is a very strong, but time consuming wrapper technique (Aha and Bankert, 1996). The idea is to start by selecting each feature individually, train for each of them a classifier and evaluate its performance using cross-validation. The feature that maximizes the performance criterion is retained. In the next step, all possible pairs comprising the first retained feature and one other feature are selected, used for training, and evaluated. The best pair is now retained, all triplets are formed, and so on. This continues until the performance does not increase anymore, or a maximum number of features is reached. If we would not work with the reflectance ratios, the SFS algorithm can be easily used to sequentially select the best 8 wavelengths, since a single feature then corresponds to a single wavelength. In our case, however, selecting a feature means selecting a ratio of wavelengths. The SFS algorithm was therefore adapted to allow the sequential selection of the best wavelengths, while using features consisting of ratios of wavelengths. The functionality of SFS that enables to specify both a set of wavelengths that always must be included, as well as a set of wavelengths that must be excluded from the search, was used. The first iteration searches the best wavelength ratio by including all wavelengths. The second iteration searches the best ratios by including the previously selected wavelengths, and by excluding certain wavelengths such that the total number

of wavelengths is increased by exactly one. Iterations three to eight search first the best ratios by including the selected wavelengths of the previous iteration, and which increases the total number of wavelengths by exactly one. Second, it searches the best ratios by including the selected wavelengths of 2 iterations ago, and which increases the total number of wavelengths by exactly 2. Finally, the performance of the latter two calculations are compared and the set of features that give the best performance are retained. At the end of each iteration, additional ratios that do not increase the total number of wavelengths are also added, but only if they further improved the performance.

As a third step, the classifiers are trained, considering NB, LDA, QDA, SVM, ELM, KNN, PLS and NN. Subsequently, as in the broadband setting, the different classifiers are evaluated using 10-fold cross validation and the MCRs of each class are again combined in the single ROC metric. To obtain insight in the confidence of the developed classifiers, the variance was calculated by considering a 10 times repetition of the 10-fold cross-validation.

3. Results and discussion

We aim at linking the reflection spectroscopic data of the raw potatoes to the measured acrylamide formation during frying by using chemometrics and machine learning, while identifying the most optimal sensing wavelengths. First, insight is given in the chemical analysis results and the measured reflection spectra. Then, the different processing algorithms are compared, and their classification performance is evaluated, leading to the determination of the optimal sensing methodology.

3.1 *Chemical analysis results*

The chemical analysis of the raw potatoes and French fries gives insight in the acrylamide precursors content, and their resulting acrylamide formation after frying (Table 1). The optimally stored potatoes, sample A and B, show only low acrylamide formation during frying, below the European guidelines (European Commission, 2017). The fridge-stored potatoes, sample C, D and E, show an excessive acrylamide formation between 640 ppb and 2000 ppb. Considering the acrylamide precursors, no accurate conclusions can be drawn when considering each precursor individually. Comparing the acrylamide precursor concentrations before and after frying, a decreasing

moisture and increasing asparagine concentration can be observed for all samples. Considering the reducing sugars, a decreasing percentage is observed for sample A and B, and an increasing percentage for sample C, D and E. The determination of a correlation between the precursor concentrations and the formed acrylamide concentration is, however, hampered by the complexity of the Maillard reaction and the large variability between potato tubers. The acrylamide formation is a complex process that can follow different paths (Parker et al., 2012). This is also reflected in the chemical analysis, when comparing the precursor concentrations of the raw potatoes. Sample C and D show a comparable asparagine concentration, but sample D shows a higher acrylamide concentration due to its higher reducing sugar content. In contrast, sample E shows a high asparagine content in combination with a lower reducing sugar concentration. Consequently, only small differences in acrylamide precursors concentrations lead to extensive differences in acrylamide formation, indicating the need for a sensitive and accurate potato quality evaluation tool.

Table 1: Substituents concentrations of the analysed raw potatoes and French fries.

	Sample A		Sample B		Sample C		Sample D		Sample E	
	Raw potato	French fries	Raw potato	French fries	Raw potato	French fries	Raw potato	French fries	Raw potato	French fries
Fructose (%)	0.10	<0.05	0.05	<0.05	0.07	0.26	0.30	0.40	0.06	1.00
Glucose (%)	0.10	<0.05	0.08	0.05	0.10	0.45	0.30	0.40	<0.05	0.90
Starch (%)	/	19.01	16.85	27.62	18.37	31.00	16.91	26.04	/	26.84
Moisture (%)	76.27	52.53	77.38	51.64	73.05	46.76	75.20	48.92	72.90	47.78
Asparagine (%)	5.25	7.05	0.48	1.18	0.56	0.99	0.50	1.00	2.93	6.53
Acrylamide (ug/kg)	/	200	/	240	/	640	/	890	/	2000

3.2 Reflection spectra

The measured reflection spectra of the raw potato batches, giving rise to different acrylamide levels after frying, show in general similar absorption bands (Figure 2). A first absorption dip can be identified within the 400 – 525 nm wavelength range, induced by a combination of different potato constituents, including lutein, a pigment showing a strong absorbance between 440 – 480 nm, and riboflavin, a vitamin exhibiting a large absorbance between 400 – 500 nm (Gross, 1991; Krinsky, 2002; Orlowska et al., 2013). To date, only preliminary interpretations of the relationship between the 400 – 600 nm wavelength region, the internal potato composition and the acrylamide formation were presented (Segtnan et al., 2006; Singh, 2005). Singh presented similar optical spectra and stated that the 400 – 699 nm wavelength range can be used for the quality determination of potatoes,

allowing to differentiate between shrivelled and non-shrivelled potatoes. Segtnan et al. observed that the 400 – 600 nm wavelength range might be related to the acrylamide concentration in potato crisps. The NIR wavelength range, on the other hand, indicates the typical absorbance of reducing sugars, starch and water at 980 nm, 1220 nm and 1440 nm respectively, all of which are known as acrylamide precursors influencing the Maillard reaction.

Based on a visual interpretation of the potato spectra, no clear contrast between the potato batches can be deduced. Although some interesting spectral features can be identified, as the variation of the local maxima between 450 nm and 488 nm, no consistent change can be identified when taking the acrylamide generation into account. For example, in this wavelength range, the reflectance of the samples inducing high acrylamide contents are encapsulated by the spectra of the good potato samples, sample A and B. Within the 525 – 1700 nm range, the mean spectra of the potato samples inducing the lowest (200 ppb) and highest acrylamide content (2000 ppb) are quasi perfectly coinciding. As indicated by the chemical analysis, a direct interpretation is hampered by the variability of the acrylamide precursors and the complexity of the Maillard reaction. Therefore, there is a clear need for a robust classification algorithm retrieving the minor spectral variation between the sample batches, while dismissing the large natural variation and harvest-dependent influences.

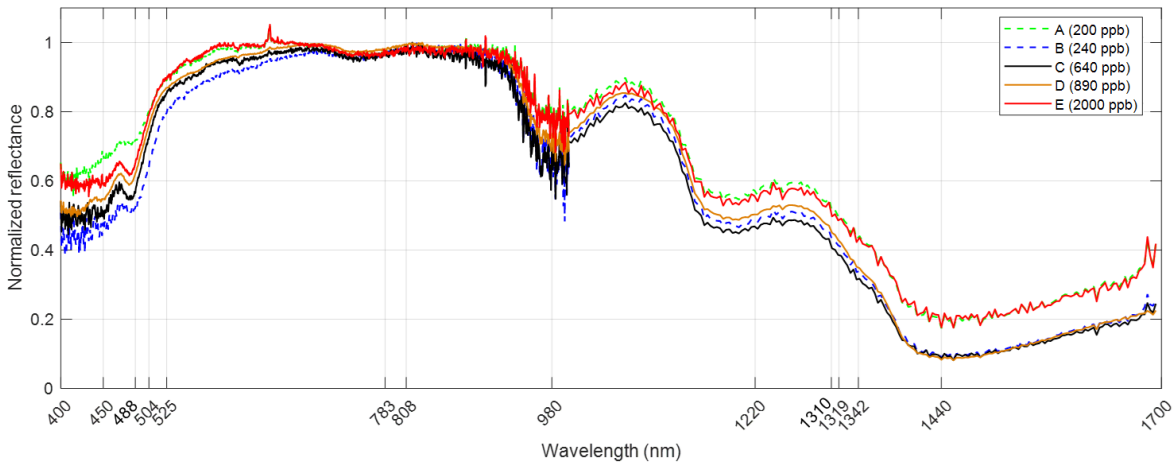

Figure 2: Normalized mean reflection spectra of the raw potatoes according to their acrylamide level after frying. The raw potatoes inducing low acrylamide content during frying (sample A, B) are indicated by dashed lines. The spectra of the raw potatoes inducing high acrylamide contents (sample C, D, E) are completely entangled with the spectra of the good ones.

3.3 Classification based on broadband spectral evaluation

The processing of broadband spectral data is often performed using PCA. With this analysis technique, a clear separation between the outer product batches, the raw potatoes inducing 200 – 240 ppb and 2000 ppb, can be observed (Figure 3). The raw potatoes inducing 890 ppb acrylamide show a minor overlap with the healthy batches, while the potatoes inducing 640 ppb completely coincide with the healthy samples hampering a correct classification. Consequently, the obtained classification is insufficient, motivating the need for more advanced data processing.

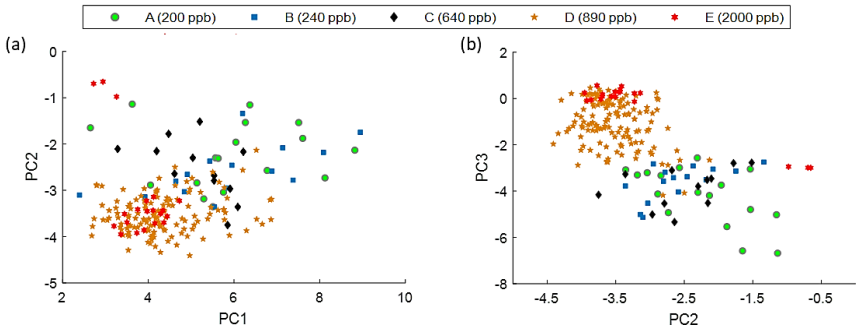

Figure 3: PCA performed on raw potato spectra indicating a clear separation between batch A-B and E, but an insufficient classification of samples C and D: (a) PC2 as function of PC1; (b) PC3 as function of PC2.

As explained in section 2.3.1, several chemometric and machine learning classifiers were trained, after application of different pre-processing techniques. Ten-fold cross-validation and the ROC metric were used to evaluate the performance of the classifiers. In general, a satisfying performance is obtained, indicating different possibilities to obtain a perfect classification on the validation sets (Figure 4). Best results were obtained using the LDA classifier, while the ELM, PLS and NN classifiers also indicated satisfying performances. The best performing PLS algorithm made use of 11 principal components. Considering the raw data, perfect classification can be obtained using the LDA and ELM classifiers. Even though the ELM classifier did not overfit (overfitting only occurs for >150 neurons, while we use 50 neurons), we would recommend using the simpler and linear LDA classifier in practice. In contrast, the QDA was generally the worst performing classifier. This is because the covariance matrix is singular when using all features, since pseudo-inverse had to be used in the algorithm, which is not a satisfying approximation of the inverse when the number of features is significantly larger than the number of measurements. Evaluating the influence of the pre-processing techniques on the general performance, for each of the classifiers, the use of SNV and MSC generally led to the most satisfying results. The performance of the

NB classifiers is the most susceptible to the applied pre-processing technique, while the LDA barely indicates any influence of the pre-processing. The superior performance of LDA originates from the fact that the features in every class approximately follow a multivariate normal distribution, each of them with a different mean but with a similar covariance.

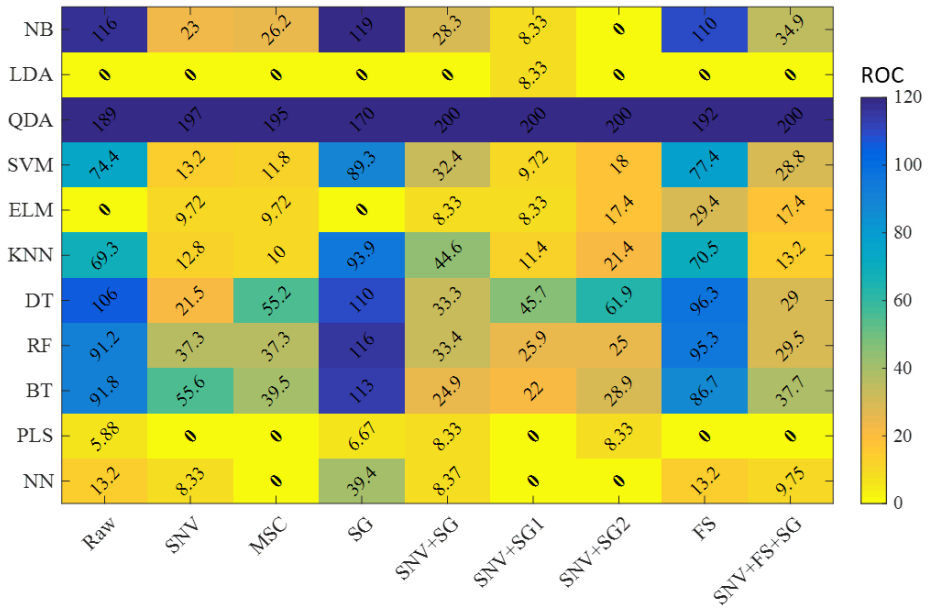

Figure 4: Classification performance evaluation of the validation sets using the ROC metric, when considering the broadband spectra. Each row corresponds to a classification algorithm, while each column represents a pre-processing technique. Optimal classification is obtained for ROC values equal to zero (indicated in bold), indicating LDA as the best classifier.

3.4 Classification based on selected wavelengths evaluation

In the next step, the classification was re-evaluated when limiting the number of wavelengths to 8, by application of our above described SFS wrapper method. This selection algorithm indicated 450/783 nm, 488/505 nm, 488/808 nm, 504/488 nm, 504/783 nm, 504/1319 nm, 783/450 nm, 783/808 nm, 808/450 nm, 808/783 nm, 1310/450 nm, 1310/505 nm, 1319/1342 nm and 1342/808 nm as key ratios. Consequently, this also implies that 450 nm, 488 nm, 504 nm, 783 nm, 808 nm, 1310 nm, 1319 nm and 1342 nm can be considered as the 8 most significant wavelengths. Looking back to the reflection spectra (Figure 2), these wavelengths also coincide with the main spectral characteristics that are linked to the acrylamide formation. Next, the reflectance ratios were considered as input for the classifiers, without any further pre-processing.

Comparing the ROC metric of the different classifiers, optimal performance was obtained using LDA (Figure 5), indicating that the ratio of reflectances can be sufficiently well approximated by a multivariate Gaussian distribution, with the same covariance for the different classes. The NN classifier showed the second-best performance, while the KNN classifier showed the worst performance.

Considering the LDA classification, the classification rates are presented in Table 2. Since the sample size did not allow for a reliable external validation and to verify if these results give a quasi-unbiased estimate of the complete model building procedure, nested cross-validation was also applied for this final model. In this technique, both the selection of the hyperparameters (none in this case of LDA) and the selection of the features (using the modified SFS) is done inside the cross-validation procedure. The inner and outer loop consisted of 5 and 10 folds respectively. The results of the nested cross-validation were very similar (within a few percent) to the results of the standard cross-validation, showing that little bias is present. This is as expected, since the SFS procedure already includes evaluation using cross-validation.

In general, a satisfying classification is obtained, indicating classification performances exceeding 92%. Sample A and E, with the lowest and highest acrylamide concentrations respectively, were perfectly classified. Sample C, inducing 640 ppb acrylamide during frying, shows the highest rate of misclassification. These misclassified samples, however, ended up in the 890 ppb class, which is a safe misclassification from a food safety point of view. This was also observed for the other samples, where the misclassified potatoes were also generally identified as having a higher acrylamide content. Only 1.5% of the samples was classified as being a good potato, while they induce excessive acrylamide formation. As far as we know, this is significantly better than what can be achieved using the current potato quality evaluation tools. Furthermore, the misclassifications might originate from the discrepancy between the chemical analysis, which measure the mean contamination level of a batch, and the optical measurements that measure the local contamination on the product. Locally, the samples might show lower or higher contamination levels, resulting in a deviating classification.

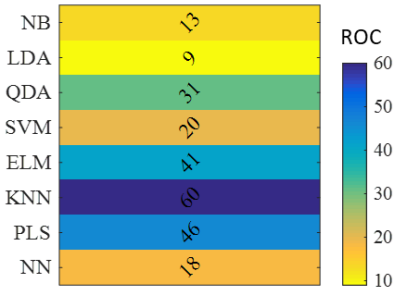

Figure 5: Classifier performance evaluation using the ROC metric, when considering 8 wavelengths. The LDA algorithm yields the best performance.

Table 2: Mean confusion matrix presenting the classification when applying LDA, when considering 10 different repeated 10-fold cross-validation runs. The error is a 95% confidence interval calculated using the standard error of the mean.

		Classification percentage				
		200 ppb	240 ppb	640 ppb	890 ppb	2000 ppb
Potato sample	A (200 ppb)	100.0 ± 0.0 %	0.0 ± 0.0 %	0.0 ± 0.0 %	0.0 ± 0.0 %	0.0 ± 0.0 %
	B (240 ppb)	0.0 ± 0.0 %	98.7 ± 0.7 %	0.7 ± 0.7 %	0.7 ± 0.7 %	0.0 ± 0.0 %
	C (640 ppb)	0.0 ± 0.0 %	0.0 ± 0.0 %	91.7 ± 0.0 %	8.3 ± 0.0 %	0.0 ± 0.0 %
	D (890 ppb)	0.0 ± 0.0 %	1.5 ± 0.0 %	2.4 ± 0.3 %	96.1 ± 0.3 %	0.0 ± 0.0 %
	E (2000 ppb)	0.0 ± 0.0 %	0.0 ± 0.0 %	0.0 ± 0.0 %	0.0 ± 0.0 %	100.0 ± 0.0 %

4. Conclusion

We demonstrated the use of reflection spectroscopy (400 – 1700 nm) combined with machine learning as a successful optical detection technique for the identification of raw potatoes giving rise to an excessive acrylamide formation during frying. A clear classification between potato batches giving rise to low (<500 ppb) and high (≥500 ppb) acrylamide concentrations during frying and complying with the European regulations was obtained. Considering the broadband reflection spectrum, an optimal classification could be obtained using Linear Discriminant Analysis or Extreme Learning Machine, without any data pre-processing and using cross-validation. Next, the machine learning processing was performed taking the constraints regarding the practical implementation into account. First, the use of a machine learning based feature selection algorithm was demonstrated to identify the most relevant wavelengths, enabling data reduction while easing the industrial integration. The eight most relevant wavelengths were identified, being 450 nm, 488 nm, 504 nm, 783 nm, 808 nm, 1310 nm, 1319 nm and 1342 nm. The reflectance values at these wavelengths contain the combined effect of the different acrylamide precursors, resulting in a harvest-independent algorithm coping with the large natural

variation in the potato batches. When only considering the reflectance values at these commercially available wavelengths, a classification performance exceeding 92 % could be obtained using Linear Discriminant Analysis. This implies that when considering an unknown raw potato, our machine learning processing enables to successfully estimate the acrylamide formation during frying based on the reflection spectroscopic properties of the raw sample. Only 1.5% of the potatoes inducing high acrylamide contents during frying was wrongfully identified as a good quality potato. In addition, and in contrast to the colour evaluation of the French fries, our novel method only requires a non-destructive food evaluation, enabling that the unsuited potatoes for frying can still be used for low-temperature processing that does not suffer from the Maillard reaction, thus limiting food waste. As a result, we believe that this research paves the way to a non-destructive identification of potatoes unsuited for French fries production, without affecting their taste, structure, colour or composition.

Acknowledgements

This work was supported in part by FWO, IWT, the MP1205 COST Action, the Methusalem and Hercules foundations and the OZR of the Vrije Universiteit Brussel (VUB). The authors would also like to thank Dr. Ir. Cédric Meshia Oveneke for his valuable input and advices regarding the applied machine learning algorithms.

References

Adedipe, O.E., Johanningsmeier, S.D., Truong, V. Den, Yencho, G.C., 2016. Development and Validation of a Near-Infrared Spectroscopy Method for the Prediction of Acrylamide Content in French-Fried Potato. J. Agric. Food Chem. 64, 1850–1860. https://doi.org/10.1021/acs.jafc.5b04733

Aha, D.W., Bankert, R.L., 1996. A comparative Evaluation of Sequential Feature Selection Algorithms, in: Fisher, D., Lenz, H.-J. (Eds.), Learning from Data: Artificial Intelligence and Statistics V. Springer, Verlag New York, pp. 199–206. https://doi.org/10.1007/978-1-4612-2404-4

Ayvaz, H., Plans, M., Riedl, K.M., Schwartz, S.J., Rodriguez-Saona, L.E., 2013. Application of infrared microspectroscopy and chemometric analysis for screening the acrylamide content in potato chips. Anal. Methods 5, 2020–2027. https://doi.org/10.1039/c3ay00020f

428 Barbon, S., Costa Barbon, A.P.A. Da, Mantovani, R.G., Barbin, D.F., 2018. Machine Learning Applied to Near-
429 Infrared Spectra for Chicken Meat Classification. J. Spectrosc. 2018.
430 https://doi.org/10.1155/2018/8949741

431 Bizzani, M., William Menezes Flores, D., Alberto Colnago, L., David Ferreira, M., 2020. Monitoring of soluble
432 pectin content in orange juice by means of MIR and TD-NMR spectroscopy combined with machine
433 learning. Food Chem. 332, 127383. https://doi.org/10.1016/j.foodchem.2020.127383

434 Brownlee, J., 2014. Assessing and Comparing Classifier Performance with ROC Curves [WWW Document].
435 Mach. Learn. Mastery. URL https://machinelearningmastery.com/assessing-comparing-classifier-
436 performance-roc-curves-2/ (accessed 11.23.20).

437 Brunt, K., Smits, B., Holthuis, H., 2010. Design, construction, and testing of an automated NIR in-line analysis
438 system for potatoes. Part II. Development and testing of the automated semi-industrial system with in-line
439 NIR for the characterization of potatoes. Potato Res. 53, 41–60. https://doi.org/10.1007/s11540-010-9148-
440 z

441 Büning-Pfaue, H., 2003. Analysis of water in food by near infrared spectroscopy. Food Chem. 82, 107–115.
442 https://doi.org/10.1016/S0308-8146(02)00583-6

443 Curcio, J.A., Petty, C.C., 1951. The near infrared absorption spectrum of liquid water. J. Opt. Soc. Am. 41, 302–
444 304. https://doi.org/https://doi.org/10.1364/JOSA.41.000302

445 De Wilde, T., De Meulenaer, B., Mestdagh, F., Govaert, Y., Vandeburie, S., Ooghe, W., Fraselle, S.,
446 Demeulemeester, K., Van Peteghem, C., Calus, A., Degroodt, J.M., Verhé, R., 2005. Influence of storage
447 practices on acrylamide formation during potato frying. J. Agric. Food Chem. 53, 6550–6557.
448 https://doi.org/10.1021/jf050650s

449 EFSA, 2015. Acrylamide in food is a public health concern [WWW Document]. URL
450 https://www.efsa.europa.eu/en/press/news/150604 (accessed 11.24.20).

451 European Commission, 2017. Establishing mitigation measures and benchmark levels for the reduction of the
452 presence of acrylamide in food. Off. J. Eur. Union 2158.

453 Gautam, R., Vanga, S., Ariese, F., Umapathy, S., 2015. Review of multidimensional data processing approaches

for Raman and infrared spectroscopy. EPJ Tech. Instrum. 2, 8. https://doi.org/10.1140/epjti/s40485-015-0018-6

Gökmen, V., Palazoglu, T.K., Senyuva, H.Z., 2006. Relation between the acrylamide formation and time-temperature history of surface and core regions of French fries. J. Food Eng. 77, 972–976. https://doi.org/https://doi.org/10.1016/j.jfoodeng.2005.08.030

Gorry, P.A., 1990. General Least-Squares Smoothing and Differentiation by the Convolution (Savitzky-Golay) Method. Anal. Chem. 62, 570–573. https://doi.org/10.1021/ac00205a007

Gross, J., 1991. Carotenoid distribution in vegetables, in: Pigments in Vegetables: Chlorophylls and Carotenoids. Springer Science + Business Media, New York, pp. 148–249. https://doi.org/10.1007/978-1-4615-2033-7

Hebeisen, T., Ballmer, T., Reust, W., 2007. Influence of storage temperature of potatoes on acrylamide formation in roasted dishes. Acta Hortic. 745, 387–392. https://doi.org/10.17660/ActaHortic.2007.745.24

Helgerud, T., Segtnan, V.H., Wold, J.P., Ballance, S., Knutsen, S.H., Rukke, E.O., Afseth, N.K., 2012. Near-infrared spectroscopy for rapid estimation of dry matter content in whole unpeeled potato tubers. J. Food Res. 1, 55–65. https://doi.org/10.5539/jfr.v1n4p55

Helgerud, T., Wold, J.P., Pedersen, M.B., Liland, K.H., Ballance, S., Knutsen, S.H., Rukke, E.O., Afseth, N.K., 2015. Towards on-line prediction of dry matter content in whole unpeeled potatoes using near-infrared spectroscopy. Talanta 143, 138–144. https://doi.org/10.1016/j.talanta.2015.05.037

Integrated Optics, 2020. CW Lasers [WWW Document]. URL https://integratedoptics.com/products/cw-lasers (accessed 10.24.20).

Jung, M.Y., Choi, D.S., Ju, J.W., 2003. A novel technique for limitation of acrylamide formation in fried and baked corn chips and in French fries. J. Food Sci. 68, 1287–1290. https://doi.org/10.1111/j.1365-2621.2003.tb09641.x

Krinsky, N.I., 2002. Possible biologic mechanisms for a protective role of xanthophylls. J. Nutr. 132, 540–542. https://doi.org/10.1093/jn/132.3.540S

Linsinska, G., Leszczynski, W., 1989. Potato storage, in: Potato Science and Technology. Springer Science & Business Media, London, pp. 129–161.

Lopez, A., Arazuri, S., Garcia, I., Mangado, J., Jaren, C., Accepted, J., 2013. A Review on the Application of Near-Infrared Spectroscopy for the Analysis of Potatoes. J. Agric. Food Chem. 61, 5413−5424. https://doi.org/10.1021/jf401292j

Matsuura-Endo, C., Ohara-Takada, A., Chuda, Y., Ono, H., Yada, H., Yoshida, M., Kobayashi, A., Tsuda, S., Takigawa, S., Noda, T., Yamauchi, H., Mori, M., 2006. Effects of storage temperature on the contents of sugars and free amino acids in tubers from different potato cultivars and acrylamide in chips. Biosci. Biotechnol. Biochem. 70, 1173–1180. https://doi.org/https://doi.org/10.1271/bbb.70.1173

Medeiros, R. V., Mestdagh, F., De Meulenaer, B., 2012. Acrylamide formation in fried potato products - Present and future, a critical review on mitigation strategies. Food Chem. 133, 1138–1154. https://doi.org/10.1016/j.foodchem.2011.08.001

Morales, G., Jimenez, M., Garcia, O., Mendoza, M.R., Beristain, C.I., 2014. Effect of natural extracts on the formation of acrylamide in fried potatoes. LWT - Food Sci. Technol. 58, 587–593. https://doi.org/10.1016/j.lwt.2014.03.034

Mottram, D.S., Wedzicha, B.L., Dodson, A.T., 2002. Acrylamide is formed in the Maillard reaction. Nature 419, 448–449. https://doi.org/10.1038/419448a

Mousavi Khaneghah, A., Fakhri, Y., Nematollahi, A., Seilani, F., Vasseghian, Y., 2020. The Concentration of Acrylamide in Different Food Products: A Global Systematic Review, Meta-Analysis, and Meta-Regression. Food Rev. Int. 1–19. https://doi.org/10.1080/87559129.2020.1791175

National Institute of Standards and Technology, 2020. L-Asparagine [WWW Document]. URL http://webbook.nist.gov/cgi/inchi?ID=C70473&Mask=400 (accessed 11.24.20).

Nawrocka, A., Lamorska, J., 2013. Determination of food quality by using spectroscopic methods, in: Grundas, S., Stepniewski, A. (Eds.), Advances in Agrophysical Research. InTech, Rijeka, pp. 347–368. https://doi.org/10.5772/52722

Orlowska, M., Koutchma, T., Grapperhaus, M., Gallagher, J., Schaefer, R., Defelice, C., 2013. Continuous and

pulsed ultraviolet light for nonthermal treatment of liquid foods. Part 1: Effects on quality of fructose solution, apple juice, and milk. Food Bioprocess Technol. 6, 1580–1592. https://doi.org/10.1007/s11947-012-0779-8

Ozaki, Y., McClure, W.F., Christy, A.A., 2007. Near-infrared spectroscopy in food science and technology. John Wiley & Sons, Inc., New Jersey. https://doi.org/10.1002/0470047704

Parker, J.K., Balagiannis, D.P., Higley, J., Smith, G., Wedzicha, B.L., Mottram, D.S., 2012. Kinetic model for the formation of acrylamide during the finish-frying of commercial French fries. J. Agric. Food Chem. 60, 9321–9331. https://doi.org/10.1021/jf302415n

Pedreschi, F., Kaack, K., Granby, K., Troncoso, E., 2007. Acrylamide reduction under different pre-treatments in French fries. J. Food Eng. 79, 1287–1294. https://doi.org/10.1016/j.jfoodeng.2006.04.014

Pedreschi, F., Segtnan, V.H., Knutsen, S.H., 2010. On-line monitoring of fat, dry matter and acrylamide contents in potato chips using near infrared interactance and visual reflectance imaging. Food Chem. 121, 616–620. https://doi.org/10.1016/j.foodchem.2009.12.075

Rady, A.M., Guyer, D.E., Kirk, W., Donis-González, I.R., 2014. The potential use of visible/near infrared spectroscopy and hyperspectral imaging to predict processing-related constituents of potatoes. J. Food Eng. 135, 11–25. https://doi.org/10.1016/j.jfoodeng.2014.02.021

Rong, D., Wang, H., Ying, Y., Zhang, Z., Zhang, Y., 2020. Peach variety detection using VIS-NIR spectroscopy and deep learning. Comput. Electron. Agric. 175, 105553. https://doi.org/10.1016/j.compag.2020.105553

Segtnan, V.H., Kita, A., Mielnik, M., Jørgensen, K., Knutsen, S.H., 2006. Screening of acrylamide contents in potato crisps using process variable settings and near-infrared spectroscopy. Mol. Nutr. Food Res. 50, 811–817. https://doi.org/10.1002/mnfr.200500260

Singh, B., 2005. Visible and near-infrared spectroscopic analysis of potatoes. pp. 22–89.

Smeesters, L., Meulebroeck, W., Raeymaekers, S., Thienpont, H., 2017. Internal scattering as an optical screening method to identify peeled potatoes giving rise to an excess of acrylamide. J. Food Eng. 195, 255–261. https://doi.org/10.1016/j.jfoodeng.2016.09.030

Subedi, P.P., Walsh, K.B., 2009. Assessment of potato dry matter concentration using short-wave near-infrared spectroscopy. Potato Res. 52, 67–77. https://doi.org/10.1007/s11540-008-9122-1

Voss, R.E., Baghott, K.G., Timm, H., 2015. Proper environment for potato storage, Vegetable Research and Information Center.

Zareef, M., Chen, Q., Hassan, M.M., Arslan, M., Hashim, M.M., Ahmad, W., Kutsanedzie, F.Y.H., Agyekum, A.A., 2020. An Overview on the Applications of Typical Non-linear Algorithms Coupled With NIR Spectroscopy in Food Analysis. Food Eng. Rev. 12, 173–190. https://doi.org/10.1007/s12393-020-09210-7